Genetically encoded fluorescent reporters of protein tyrosine kinase activities in living cells

Alice Y. Ting*, Kristin H. Kain†, Richard L. Klemke†, and Roger Y. Tsien*‡§

*Department of Pharmacology, ‡Howard Hughes Medical Institute, and Department of Chemistry and Biochemistry, University of California at San Diego, La Jolla, CA 92093; and †Department of Immunology, The Scripps Research Institute, La Jolla, CA 92037

The complexity and specificity of many forms of signal transduction are widely believed to require spatial compartmentation of protein kinase and phosphatase activities, yet existing methods for measuring kinase activities in cells lack generality or spatial or temporal resolution. We present three genetically encoded fluorescent reporters for the tyrosine kinases Src, Abl, and epidermal growth factor (EGF) receptor. The reporters consist of fusions of cyan fluorescent protein (CFP), a phosphotyrosine binding domain, a consensus substrate for the relevant kinase, and yellow fluorescent protein (YFP). Stimulation of kinase activities in living cells with addition of growth factors causes 20–35% changes in the ratios of yellow to cyan emissions because of phosphorylation-induced changes in fluorescence resonance energy transfer (FRET). Platelet-derived growth factor (PDGF) stimulated Abl activity most strongly in actin-rich membrane ruffles, supporting the importance of this tyrosine kinase in the regulation of cell morphology. These results establish a general strategy for nondestructively imaging dynamic protein tyrosine kinase activities with high spatial and temporal resolution in single living cells.

Phosphorylation is the most important way that individual proteins are posttranslationally modified to modulate their functions. To study kinase and phosphatase functions, methods are needed to image not only their localization but also their *activities* inside living cells. A few techniques of limited usefulness have been proposed for protein serine/threonine kinases, as reviewed in the accompanying paper (1), but even fewer exist for tyrosine kinases. Antiphosphotyrosine antibodies (2) or incorporation of radioactive phosphate from γ-labeled ATP are very useful in destructive assays with kinases purified from cells, but by themselves are of little or no use in unfractionated living cells. Imaging of fluorescence resonance energy transfer (FRET) from green fluorescent protein (GFP)-tagged proteins to acceptor-labeled phosphorylation-specific antibodies (3, 4) offers spatial resolution and greater specificity for the tagged substrate, but is still a destructive assay requiring membrane permeabilization or microinjection. In special cases where a natural protein or domain undergoes a significant conformational change on phosphorylation, fusion of two GFP mutants to both ends can yield phosphorylation-sensitive FRET (5). General methods are therefore still needed to nondestructively visualize the dynamics of activation of any tyrosine kinase or phosphatase in the genome. Here, we describe a class of FRET-based indicators that are genetically encoded (allowing for simple transfection rather than microinjection, and facile targeting to cellular compartments) and have a general design that can be extended in principle to most of the protein tyrosine kinases.

In our design, the kinase to be monitored phosphorylates an appropriate substrate peptide sequence, whereupon the concatenated phosphoamino acid binding domain intramolecularly complexes the phosphorylated peptide to create a larger and more reliable conformational change than the peptide alone would give (Fig. 1*a*). This conformational change alters the distance and/or relative orientation between the cyan and yellow fluorescent proteins [CFP and YFP (citrine), respectively] to generate a FRET change. Dephosphorylation of the peptide by a phosphatase reverses the FRET change. Analogous concatenations of interacting polypeptide domains bracketed by two colors of fluorescent proteins are proving useful for monitoring many other ligands and conformational changes (6–10), including phosphorylation of serine residues by protein kinase A (1). We prepared phosphorylation indicators with consensus peptide sequences for three different tyrosine kinases: Src, epidermal growth factor receptor (EGFR), and Abl (Fig. 1*b*). These three tyrosine kinases represent key components of the two growth factor-stimulated signaling pathways depicted in Fig. 1*c* and illustrate the generality of the technique for monitoring both soluble and membrane-bound receptor tyrosine kinases. The phosphotyrosine binding domain SH2 (Src homology domain 2) was used for the construction of the Src and EGFR tyrosine kinase indicators (11). The Abl indicator is derived from the endogenous protein Crk, which has its own SH2 domain and Abl phosphorylation site ready to form an intramolecular complex on tyrosine phosphorylation (12, 13).

Characterization of all three indicators both *in vitro* and in cultured mammalian cells demonstrated 20–35% changes in yellow to cyan emission ratios on stimulation of the corresponding kinase activities. In addition, by using the Abl indicator, we demonstrated dramatic spatial and temporal localization of Abl activity to actin-rich membrane ruffles after platelet-derived growth factor (PDGF) stimulation in NIH 3T3 cells. These results establish a general and noninvasive strategy for imaging tyrosine kinase activities in living cells that should be extensible to nearly all of the proteins in the tyrosine kinase family.

Methods

Gene Construction. The genes for the three indicators were constructed by amplification of the cDNA of the appropriate SH2 domain by PCR with a sense primer containing an *Sph*I site and a reverse primer containing an *Sac*I site. For the EGFR indicator, the SH2 domain (residues 374–465) from mouse p52 Shc was used. The SH2 domain for the Src indicator was amplified from the Rous sarcoma virus Src gene (residues 148–245). For the Crk-based indicator, the complete chicken c-CrkII gene was incorporated. The reverse cloning primer contained the gene sequence for the linker and phosphorylation substrate regions as shown in Fig. 1*b*. The restricted products were ligated and cloned in-frame into the *Sac*I/*Sph*I sites of pYC3.3 (14) between the EYFP (enhanced YFP, or citrine) and
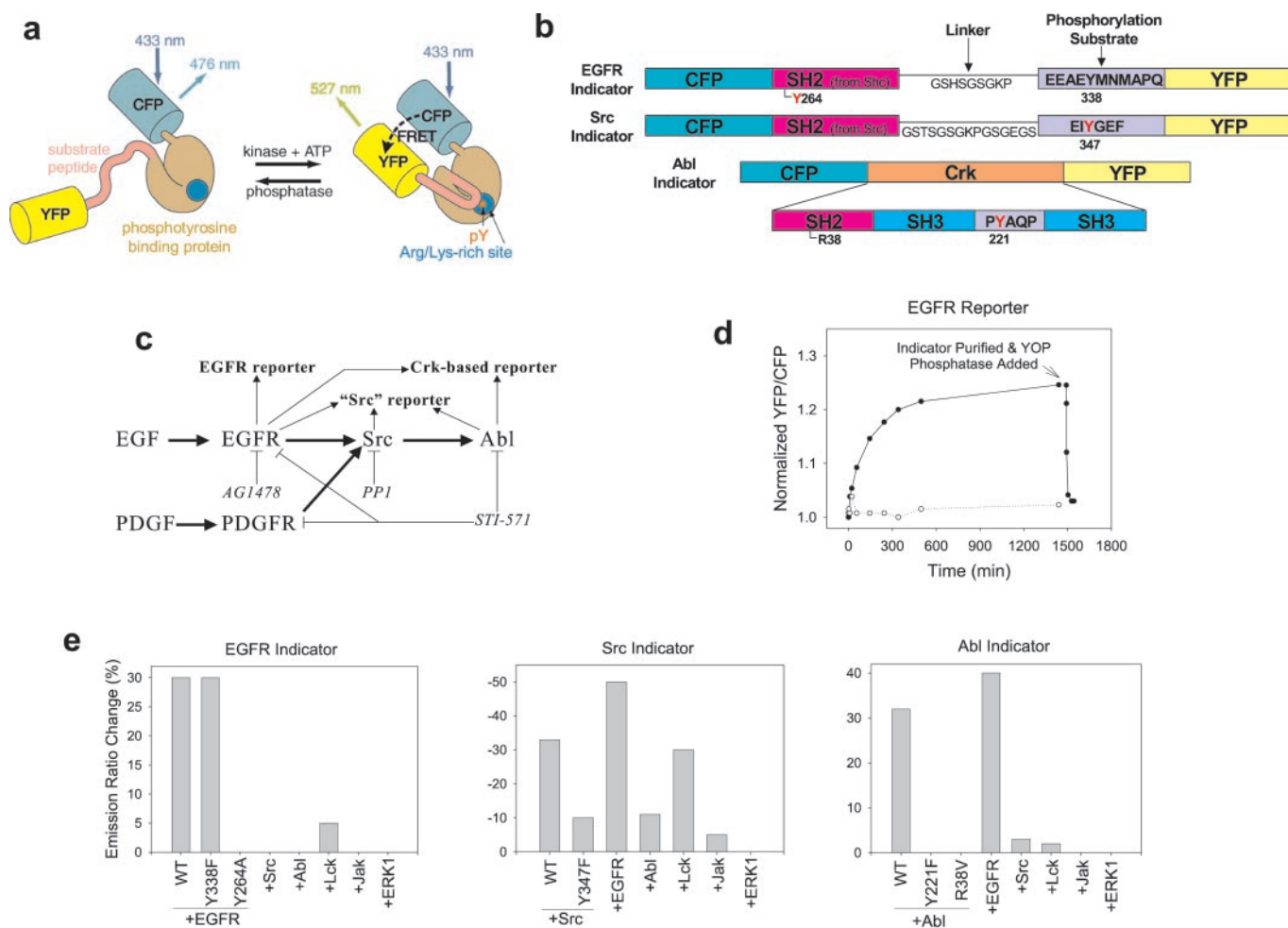
CELL BIOLOGY

Fig. 1. General design of ratiometric indicators for monitoring tyrosine kinase activities (*a*). On phosphorylation by a kinase of interest, the phosphotyrosine binding domain (such as an SH2 domain) forms an intramolecular complex with the phosphotyrosine side chain, giving rise to a distance change between the two flanking GFPs that alters the FRET. Dephosphorylation reverses the FRET change. The domain structures of the individual indicators are shown in *b*. The three tyrosine kinases lie along the growth factor-stimulated signaling pathways depicted in *c*. In the scheme, indicators are boldfaced, the major tyrosine kinases are enlarged, and kinase inhibitors are italicized. When the purified EGFR indicator was treated with EGFR kinase and ATP *in vitro*, a 25% increase in emission ratio was observed (*d*). Reversal of the FRET change was observed after removal of the kinase and addition of YOP tyrosine phosphatase (data not shown for the Src and Abl indicators). Site-directed mutagenesis was used to examine the mechanistic basis of the FRET response of each of the indicators. The percentage emission ratio change for each indicator and mutant in response to *in vitro* phosphorylation is shown in *e*. Indicator specificity was tested by using a panel of different kinases as shown in *e*.

ECFP [enhanced CFP, truncated at the C terminus (7)] genes. Site-directed mutagenesis was performed by using the QuikChange kit (Stratagene). For mammalian expression, the chimeric proteins were subcloned into pcDNA3 (Invitrogen) by using the *Hin*dIII and *Eco*RI restriction sites. All three gene sequences have been deposited with GenBank under accession numbers AF440201 (EGFR reporter), AF440202 (Src reporter), and AF440203 (Crk-based reporter).

Protein Expression, *in Vitro* Spectroscopy, and Phosphorylation Reactions. Chimeric proteins were expressed as N-terminal His$_6$ tag fusions in *Escherichia coli* as previously described (15). Emission ratios (526 nm/476 nm) were measured in a cuvette with excitation at 434 nm as purified indicators were phosphorylated with purified kinases [EGFR + EGF from Sigma, c-Src and Jak2 from Upstate Biotechnology (Lake Placid, NY), and c-Abl from Calbiochem] in the presence of 0.1–1 mM ATP at 25°C. For dephosphorylation assays, the His$_6$-tagged indicators were first purified by Ni-NTA agarose to remove the remaining kinases

and ATP, and YOP protein tyrosine phosphatase (New England Biolabs) was added at 25°C to initiate dephosphorylation.

Cells and Antibodies. HeLa and NIH 3T3 cells were purchased from American Type Culture Collection. B82 cells were a gift from Gordon Gill (University of California, San Diego). MEF cells derived from mice genetically lacking Abl as well as the related kinase Arg, and wild-type littermate controls, were a gift from Anthony Koleske (Yale University). Anti-phosphotyrosine antibody 4G10 was purchased from Upstate Biotechnology. Anti-Crk monoclonal antibody was purchased from Transduction Laboratories (Lexington, KY). Anti-GFP rabbit polyclonal antibody was a gift from Charles Zuker (University of California, San Diego), and anti-phospho-CrkII antibody was a gift from Michiyuki Matsuda (Osaka University, Japan).

Imaging. Cells maintained in 10% fetal bovine or calf serum were transfected with Effectene (Qiagen, Chatsworth, CA) for 6–12 h, then starved in 0.2% calf serum for another 12–24 h. During imaging, cells were maintained in Hanks' balanced salt solution

(HBSS) with 20 mM Hepes (pH 7.4) and 2 g/liter D-glucose at 25°C. Images were collected as previously described (15) by using MetaFluor 2.75 software (Universal Imaging, Downington, PA) with a 440DF20 excitation filter, a 455DRLP dichroic mirror, and two emission filters (480DF30 for ECFP and 535DF25 for citrine). Kinase activities were stimulated with epidermal growth factor (EGF; 50 ng/ml) or PDGF (50 ng/ml). Kinase inhibitors were used at 100 nM (PP1 and AG1478) or 10 μM (STI-571).

Results

In Vitro Characterization. When each of the three reporters was purified from a bacterial expression system and treated with the appropriate kinase and ATP, the ratio of yellow to cyan emissions changed by 25–35% (Fig. 1d). The responses depended on phosphorylation, as leaving out the ATP or kinases abolished the FRET changes. The EGFR and Abl reporters responded with increases in FRET as designed, whereas phosphorylation decreased FRET within the Src reporter. Because the GFP units have a limited tendency to dimerize (16), perhaps the Src indicator possessed some tertiary structure that was disrupted upon phosphorylation by the kinase, leading to a FRET decrease. All in vitro FRET changes were reversed on addition of the nonspecific tyrosine phosphatase YOP, indicating that intramolecular encapsulation of the phosphotyrosine does not sterically prevent dephosphorylation, probably because of the rapid on- and off-rates of the SH2 binding domain (11). The specificity of each indicator was evaluated by testing against a panel of different kinases in vitro (Fig. 1e). The EGFR indicator was responsive to phosphorylation by EGFR, but not Src, Abl, Lck, Jak2, or the serine/threonine kinase MAPK-ERK1 (mitogen-activated protein kinase-extracellular signal-regulated kinase 1). The Crk-based indicator was responsive to both EGFR and Abl, consistent with previous reports (12, 17). The "Src" reporter was the least specific of all, giving sizeable FRET responses to phosphorylation by Src, Abl, Lck, and EGFR.

Several indicator mutants were tested to elucidate the mechanism of the FRET responses (Fig. 1e). For the Crk-based indicator, mutations in the natural Abl phosphorylation site (Y221F) and in the SH2 domain of Crk, which binds phosphorylated Y221 (R38V), confirmed that intramolecular complexation was the mechanistic basis of the FRET increase on phosphorylation by Abl. Mutation of Y347 in the consensus substrate region of the Src reporter to phenylalanine decreased the responsivity to phosphorylation, as expected, but did not abolish it, suggesting that this indicator operates partly by intramolecular complexation, and partly by another unresolved mechanism. The FRET increase in the EGFR indicator persisted despite mutation of the designed phosphorylation target Y338 to phenylalanine, showing that this molecule also operates by a mechanism requiring fuller elucidation.

EGFR Reporter in Living Mammalian Cells. In cultured mammalian cells transfected with the phosphorylation indicators, we stimulated kinases with growth factors while continuously imaging emission ratios to monitor FRET. Application of EGF to B82 mouse fibroblasts stably overexpressing EGFR (18) increased the emission ratio of the transiently expressed reporter by 25–35% over ≈3 min (Fig. 2 a and b). The yellow and cyan emission intensities were anticorrelated, consistent with a FRET mechanism (data not shown). As expected for a membrane-bound kinase and a diffusible indicator, the FRET response originated from the plasma membrane and visibly propagated throughout the cytoplasm (see Movie 1, which is published as supporting information on the PNAS web site, www.pnas.org). The FRET response could be reversed by dephosphorylation of the indicator (Fig. 2 c and d). When EGF was removed from the cells, the emission ratio returned to its original level in ≈30 min (Fig. 2d). The recovery was accelerated to <5 minutes when the

EGFR inhibitor AG1478 was added concurrently with EGF washout. This finding shows that phosphatases can very rapidly dephosphorylate the reporter in cells. The much slower decay without AG1478 suggests that EGFR remains active for up to 30 min after removal of extracellular EGF, probably because of continued activation by EGF within endocytic vesicles (19).

Several controls were performed to verify the specificity of the FRET response to EGFR activity. When the cells were pretreated with the inhibitor AG1478, or replaced by cells lacking EGFR or expressing a kinase-dead mutant of EGFR (18), no FRET change was observed (data not shown). When B82 or NIH 3T3 cells transfected with the EGFR indicator were stimulated with PDGF, no FRET change was observed. Because NIH 3T3 cells naturally express high amounts of PDGF receptor (PDGFR; ref. 20), this measurement indicates that the EGFR reporter is at least specific for phosphorylation by EGFR over both PDGFR and its downstream effectors, including Src (Fig. 1c). We also observed that the Src family inhibitor PP1, in contrast to AG1478, did not block the FRET response in B82 cells, again showing that this indicator is specific for EGFR over Src. Finally, we carried out dose–response measurements to show that the EGFR indicator is sensitive to the concentration of EGF applied. Maximal FRET response was observed with 50 ng/ml of EGF or greater, whereas concentrations <10 ng/ml gave no response. Emission ratio changes were consistently reduced by approximately one half when 25 ng/ml of EGF was used. The response time was unvaried in all cases (data not shown).

To investigate the mechanism of EGFR reporter action inside cells, we first established a correlation between the FRET response and the phosphorylation state of the indicator by immunoprecipitating the reporter from mammalian cell lysates by using an anti-GFP antibody and blotting with antibodies recognizing phosphotyrosine (Fig. 2c). We then tested the FRET response of a mutant in which the critical arginine side chain within the SH2 domain of the indicator had been mutagenized to valine, abolishing the affinity of this domain for phosphotyrosine. The elimination of the FRET response in B82 cells to EGF stimulation by this mutation (data not shown) suggests that a physical interaction between the SH2 domain of the indicator and the autophosphorylation sites in the C-terminal domain of EGFR may precede phosphorylation of the indicator by EGFR.

Cellular Response of the Src Reporter. The cellular response of the Src reporter was tested in both NIH 3T3 and HeLa cells via PDGF or EGF stimulation, respectively, of Src activity. In both cases, a 25–30% decrease in yellow to cyan emission ratio was observed, with spatial propagation from the plasma membrane to the center as with the EGFR reporter response (Fig. 2e). The FRET change was reversed when the growth factor was washed out and an appropriate kinase inhibitor was added (Fig. 2f). The FRET change could be blocked by pretreating NIH 3T3 cells with PP1. However, for HeLa cells stimulated with EGF, inhibition by PP1 was incomplete, presumably because both EGFR and Src phosphorylate the Src reporter (as suggested by the in vitro data).

Cellular Response of the Crk-Based Reporter. The involvement of Abl in cell migration has been suggested by several studies (20–23). Specifically, the phosphorylation of Crk, the central component of our reporter, by Abl is thought to play a role in focal adhesion turnover and the formation of membrane ruffles (21). Pendergast and colleagues (20) measured the localization of Abl activity in migrating NIH 3T3 cells by using cellular subfractionation followed by in vitro phosphorylation assays, and found the highest Abl activity in the membrane/cytoskeletal fraction. Direct visualization of the time course and localization
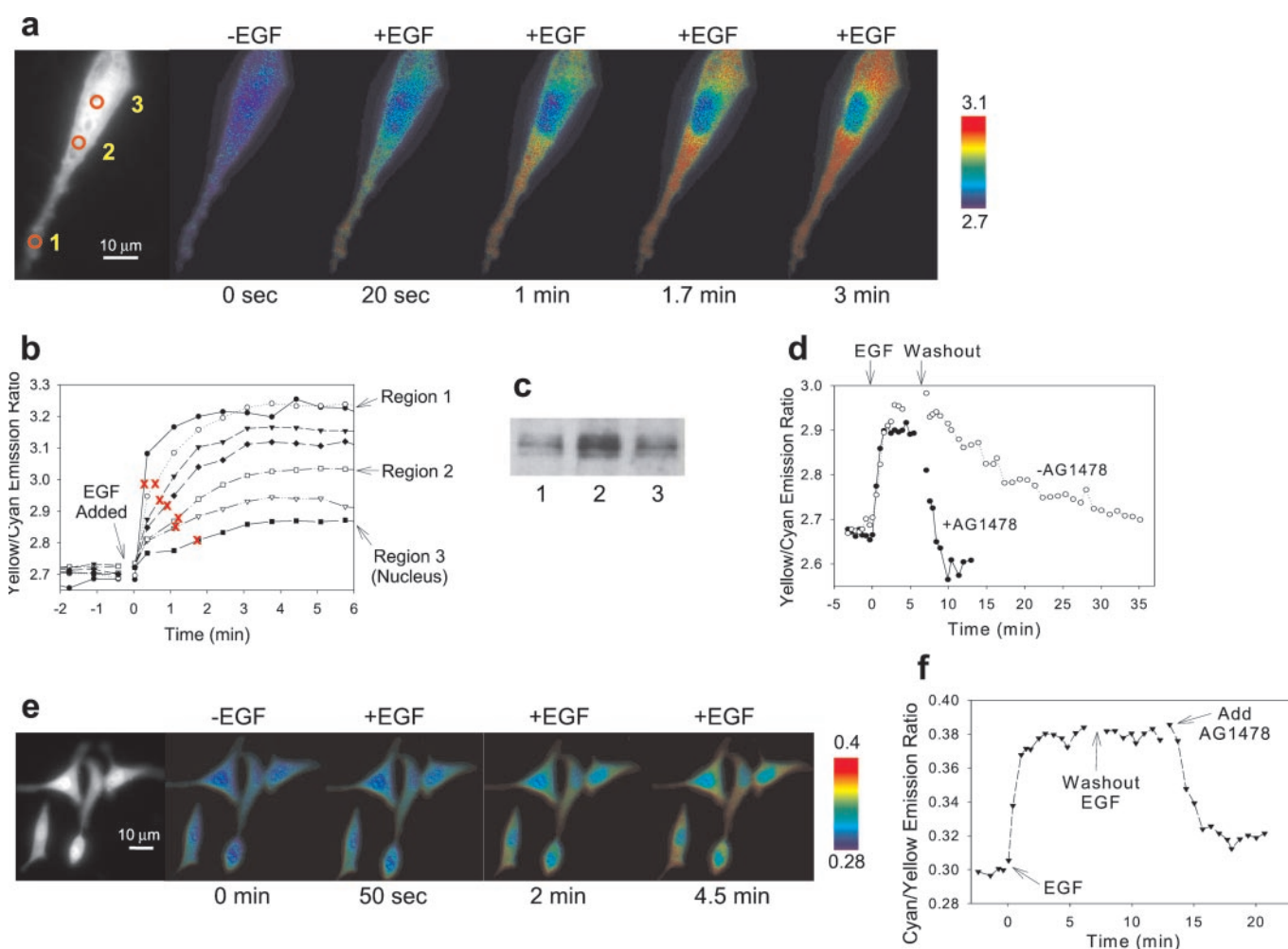
Fig. 2. B82 cells transfected with the EGFR indicator responded to EGF stimulation with an ≈30% increase in yellow to cyan emission ratio (transition from blue to red pseudocolor; *a*). The FRET change visibly propagated from the plasma membrane to the rest of the cytosol in ≈3 min. The far left shows the fluorescence from the YFP channel only. Three different subcellular regions are circled in red and correspond to the indicated lines in the time course graph shown in *b*. The red x's on the graph denote the times at which each subcellular region reached 50% of its maximal FRET change. Antiphosphotyrosine Western analysis of immunoprecipitated EGFR reporter (using α-GFP) showed an increase in phosphorylation level on EGF treatment (*c*). Lane 1, unstimulated cells; lane 2, cells treated with EGF for 10 min; lane 3, EGF treatment, followed by washout and addition of AG1478 for 20 min. The EGFR indicator was a reversible reporter (*d*). On removal of EGF, the FRET change slowly reversed to its original level in ≈30 min. Reversal was accelerated by adding the EGFR inhibitor AG1478. The FRET response of the Src reporter in HeLa cells stimulated with EGF is shown in *e*. The far left shows the YFP-only image. This indicator, too, was reversible, giving a recovery in FRET change after removal of extracellular EGF and addition of AG1478 (*f*).

of Abl activity in living cells undergoing morphological changes, however, has never been demonstrated. We therefore used our Crk-based indicator to observe the pattern of Abl activity in migrating NIH 3T3 cells stimulated with PDGF. On addition of PDGF-BB, serum-starved NIH 3T3 cells transfected with the indicator displayed a gradual 10–15% emission ratio increase over ≈20 min in the cytoplasm, consistent with an elevation in Abl activity (Fig. 3 *c* and *d*). No FRET change was observed in the nucleus. In the membrane ruffles that appeared as a typical response to PDGF stimulation, we observed concentration of the indicator and elevated FRET in comparison with all other subcellular compartments (Movie 2, which is published as supporting information on the PNAS web site; Fig. 3 *d* and *e*). The aggregation of the indicator in the ruffles may be a consequence of recruitment of the indicator to ruffles by Abl or other proteins; for instance, association between the polyproline region of Abl and the N-terminal SH3 domain of Crk has been demonstrated (12). Separate measurements verified that the emission ratio reported by the Crk-based indicator was independent of indicator concentration over the range typically

observed in transfected cells. The difference between the cytoplasmic FRET response and the FRET change in the membrane ruffles was very striking; the greatest FRET was clearly localized to the cell periphery, and the response continued to climb in the ruffles throughout the duration of PDGF stimulation (Fig. 3*c*).

Several controls were performed to verify the specificity of the Crk-based indicator in NIH 3T3 cells for phosphorylation by Abl. In cells pretreated with the Abl inhibitor STI-571 (also an inhibitor of PDGFR, however), no activation of Abl was observed in any part of the cell (data not shown). Western blot analysis of crude cell lysates confirmed the correlation between the phosphorylation state of the indicator and the measured FRET (Fig. 3*b*). Replacement of the Crk-based indicator with either of the two mutants Y221F (unphosphorylatable) or R38V (impaired SH2 domain) abolished the FRET response to PDGF addition. Moreover, we stimulated Abl activity in mouse embryonic fibroblasts (MEFs) with hydrogen peroxide, a strong activator of cytoplasmic Abl (24) and compared the response to that of genetically altered MEFs lacking Abl ($abl^{-/-}\ arg^{-/-}$). Previous studies have shown that Crk Y221 phosphorylation in
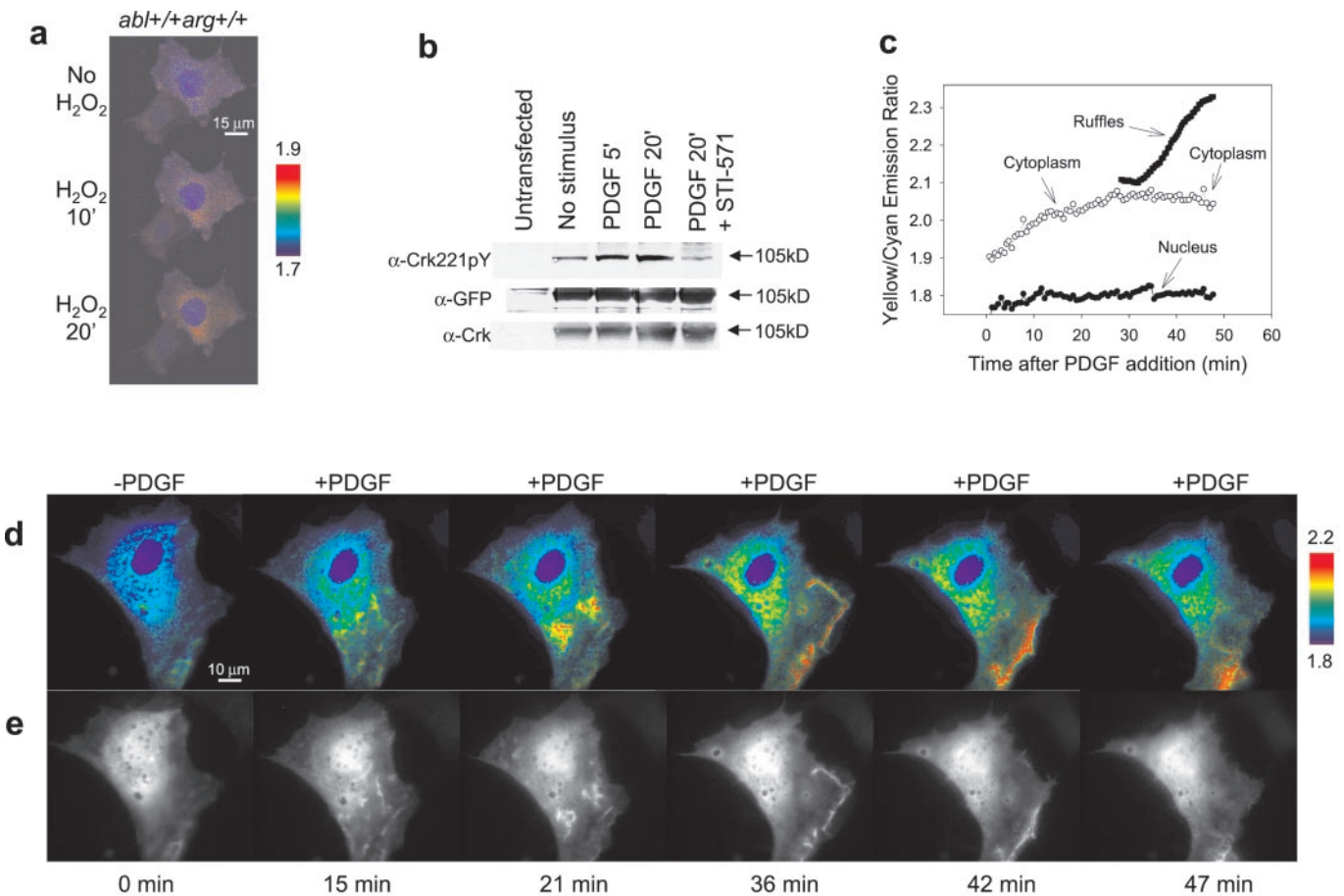
Fig. 3. Cellular response of the Crk-based reporter. Wild-type MEFs stimulated with H_2O_2 displayed a FRET increase in the cytosol over 20 min but no change in the nucleus (*a*). Null cells did not display such an increase. An antiphospho-Y221Crk Western blot of crude cell lysates from NIH 3T3 cells transfected with the Crk-based indicator shows an increase in phosphorylation of the indicator on PDGF stimulation (*b*). Phosphorylation is suppressed by pretreating cells with the Abl inhibitor STI-571. The emission ratio time course (*c*) for different regions of the PDGF-stimulated cell depicted in *d* shows a cytoplasmic increase in FRET followed by a dramatic FRET increase within the PDGF-induced membrane ruffles. Corresponding images of the YFP fluorescence show that the Abl reporter concentrates in the membrane ruffles (*e*).

these cells results specifically from Abl and/or Arg activity (21). Whereas wild-type MEFs responded to hydrogen peroxide with a 10–15% increase in yellow to cyan emission ratio (Fig. 3*a*), null cells displayed no increase, demonstrating that the indicator is specific for phosphorylation by Abl and/or Arg kinases under these conditions. PDGF stimulation of the MEFs was not successful, in that no indicator response was observed, probably because these cells display low PDGFR expression (unpublished observations).

The properties of our Crk-based indicator agree fairly well with those of a similar indicator reported by Kurokawa *et al.* (5), who found that full-length rat CrkII inserted between CFP and YFP gave very little FRET response to phosphorylation. Truncation of the rat CrkII segment was necessary to obtain a usable indicator for phosphorylation by Abl and EGFR, whereas we obtained 15–30% emission ratio changes in live cells with a slightly truncated CFP fused to the full-length chicken CrkII gene and YFP. Kurokawa *et al.* used their Crk-based indicator to measure elevated FRET in HT1080 cells expressing c-Abl as compared to cells lacking this kinase, but did not report acute stimulation of Abl activity and direct monitoring of the resulting dynamic FRET changes as we demonstrated. They did describe measurements of indicator phosphorylation by EGFR, and the results match ours in several respects. Like Kurokawa *et al.*, we saw an ≈30% increase in yellow to cyan emission ratio upon addition of EGF that was reversible and could be blocked by

preaddition of AG1478. Furthermore, we did not see any spatial heterogeneity in the cytoplasmic FRET response of the indicator to EGF stimulation, in agreement with their data. It is interesting to compare this observation with the results obtained with our EGFR indicator, with which we saw clear propagation of the FRET response from the plasma membrane to the rest of the cytosol. The primary difference between our indicator and that of Kurokawa *et al.* in response to EGF stimulation was the response time; whereas our reporter reached its maximal FRET response within 40 s of EGF addition, their reporter reached its maximal response in 10 min. This >10-fold difference in rate may be a result of the different cell lines used (B82 instead of Cos-1).

Discussion

Whereas the function of cytoplasmic Abl is not well understood, the presence of actin interaction domains in the C-terminal half of the kinase suggests a possible role in cytoskeletal regulation. Crk constitutes a particularly interesting Abl indicator, as the FRET response reports both Abl kinase activity and Crk phosphorylation. Previous studies have shown that Abl phosphorylation of Crk and the focal adhesion protein paxillin is important in cell spreading and focal contact turnover, with Crk phosphorylation instigating the disruption of Crk-associated complexes (21, 23, 25, 26). Our observation that the Crk-based indicator shows the highest FRET in the ruffles of PDGF-stimulated cells

is most simply consistent with elevated Abl activity in those ruffles, an area with a high rate of focal contact turnover (27). The alternative hypothesis that the indicator is phosphorylated elsewhere and that the ruffles selectively recruit the phosphorylated species is less likely, because the known interactions of Crk with Abl, paxillin, and PDGR are preferentially with the non-phosphorylated, open conformation of Crk (23, 28). We note that, because STI-571 also inhibits PDGFR, we cannot exclude the possibility that Crk is phosphorylated directly by PDGFR or indirectly by an Abl-independent pathway. Our results thus support the emerging role of cytoplasmic Abl as a regulator of cell morphology.

The successful creation of fluorescent indicators for EGFR, Src, and Abl and their application to the study of compartmentalized and dynamic modulation of Abl activity during cytoskeletal remodeling suggest that this general strategy for nondestructive imaging of protein tyrosine kinase activities should be extensible to many other tyrosine kinases. Our analogous success with a reporter for protein kinase A (1) shows that the generic design works for both serine/threonine and tyrosine kinases. All these surrogate phosphorylation substrates complement but do not replace measurements of the phosphorylation of endogenous substrates. But they offer precise subcellular targeting and versatile construction, as well as unmatched spatiotemporal resolution in live cells. Because most kinases have overlapping substrate specificities, each indicator's specificity and mechanism will need to be checked by biochemical, pharmacological, and genetic tests as shown above. Future generations of phosphorylation indicators may use the PTB phosphotyrosine binding domain or other natural or engineered domains instead of SH2. Domains such as FHA and WW (29) may replace 14-3-3 for binding phosphoserine or phosphothreonine. Additional recruitment motifs could also be added to indicators to enhance kinase specificity, and high throughput methods could help generate more and better indicators. Optimized indicators could be of great value in pharmaceutical screening for tyrosine kinase and phosphatase modulators, whose immense clinical potential has been exemplified by the efficacy of STI-571 (Gleevec) in treating certain leukemias.

1. Zhang, J., Ma, Y., Taylor, S. S. & Tsien, R. Y. (2001) *Proc. Natl. Acad. Sci. USA* **98,** 14997–15002.
2. Czernik, A. J., Girault, J.-A., Nairn, A. C., Chen, J., Snyder, G., Kebabian, J. & Greengard, P. (1991) *Methods Enzymol.* **201,** 264–283.
3. Verveer, P. J., Wouters, F. S., Reynolds, A. R. & Bastiaens, P. I. (2000) *Science* **290,** 1567–1570.
4. Ng, T., Squire, A., Hansra, G., Bornancin, F., Prevostel, C., Hanby, A., Harris, W., Barnes, D., Schmidt, S., Mellor, H., *et al.* (1999) *Science* **283,** 2085–2089.
5. Kurokawa, K., Mochizuki, N., Ohba, Y., Mizuno, H., Miyawaki, A. & Matsuda, M. (2001) *J. Biol. Chem.* **276,** 31305–31310.
6. Romoser, V. A., Hinkle, P. M. & Persechini, A. (1997) *J. Biol. Chem.* **272,** 13270–13274.
7. Miyawaki, A., Llopis, J., Heim, R., McCaffery, J. M., Adams, J. A., Ikura, M. & Tsien, R. Y. (1997) *Nature (London)* **388,** 882–887.
8. Miyawaki, A., Griesbeck, O., Heim, R. & Tsien, R. Y. (1999) *Proc. Natl. Acad. Sci. USA* **96,** 2135–2140.
9. Mochizuki, N., Yamashita, S., Kurokawa, K., Ohba, Y., Nagai, T., Miyawaki, A. & Matsuda, M. (2001) *Nature (London)* **411,** 1065–1068.
10. Nagai, Y., Miyazaki, M., Aoki, R., Zama, T., Inouye, S., Hirose, K., Iino, M. & Hagiwara, M. (2000) *Nat. Biotechnol.* **18,** 313–316.
11. Kuriyan, J. & Cowburn, D. (1997) *Annu. Rev. Biophys. Biomol. Struct.* **26,** 259–288.
12. Feller, S. M., Knudsen, B. & Hanafusa, H. (1994) *EMBO J.* **13,** 2341–2351.
13. Cotton, G. J. & Muir, T. W. (2000) *Chem. Biol.* **7,** 253–261.
14. Griesbeck, O., Baird, G. S., Campbell, R. E., Zacharias, D. A. & Tsien, R. Y. (2001) *J. Biol. Chem.* **276,** 29188–29194.
15. Miyawaki, A. & Tsien, R. Y. (2000) *Methods Enzymol.* **327,** 472–500.
16. Ward, W. W., Prentice, H. J., Roth, A. F., Cody, C. W. & Reeves, S. C. (1982) *Photochem. Photobiol.* **35,** 803–808.
17. Hashimoto, Y., Katayama, H., Kiyokawa, E., Ota, S., Kurata, T., Gotoh, N., Otsuka, N., Shibata, M. & Matsuda, M. (1998) *J. Biol. Chem.* **273,** 17186–17191.
18. Chen, W. S., Lazar, C. S., Poenie, M., Tsien, R. Y., Gill, G. N. & Rosenfeld, M. G. (1987) *Nature (London)* **328,** 820–823.
19. Opresko, L. K., Chang, C. P., Will, B. H., Burke, P. M., Gill, G. N. & Wiley, H. S. (1995) *J. Biol. Chem.* **270,** 4325–4333.
20. Plattner, R., Kadlec, L., DeMali, K. A., Kazlauskas, A. & Pendergast, A. M. (1999) *Genes Dev.* **13,** 2400–2411.
21. Kain, K. H. & Klemke, R. L. (2001) *J. Biol. Chem.* **276,** 16185–16192.
22. Salgia, R., Li, J. L., Ewaniuk, D. S., Pear, W., Pisick, E., Burky, S. A., Ernst, T., Sattler, M., Chen, L. B. & Griffin, J. D. (1997) *J. Clin. Invest.* **100,** 46–57.
23. Escalante, M., Courtney, J., Chin, W. G., Teng, K. K., Kim, J. I., Fajardo, J. E., Mayer, B. J., Hempstead, B. L. & Birge, R. B. (2000) *J. Biol. Chem.* **275,** 24787–24797.
24. Sun, X., Majumder, P., Shioya, H., Wu, F., Kumar, S., Weichselbaum, R., Kharbanda, S. & Kufe, D. (2000) *J. Biol. Chem.* **275,** 17237–17240.
25. Lewis, J. M. & Schwartz, M. A. (1998) *J. Biol. Chem.* **273,** 14225–14230.
26. Mayer, B. J., Hirai, H. & Sakai, R. (1995) *Curr. Biol.* **5,** 296–305.
27. Ridley, A. J. & Hall, A. (1992) *Cell* **70,** 389–399.
28. Sorokin, A., Reed, E., Nnkemere, N., Dulin, N. O. & Schlessinger, J. (1998) *Oncogene* **16,** 2425–2434.
29. Yaffe, M. B. & Elia, A. E. (2001) *Curr. Opin. Cell Biol.* **13,** 131–138.